Biochemical and Biophysical Research Communications 460 (2015) 727–732

Contents lists available at ScienceDirect

Biochemical and Biophysical Research Communications

journal homepage: www.elsevier.com/locate/ybbrc

Roles of hepatic glucokinase in intertissue metabolic communication: Examination of novel liver-specific glucokinase knockout mice

Hirofumi Hayashi [a, 1], Yoshifumi Sato [a, 1], Zhenghua Li [b], Ken-ichi Yamamura [b], Tatsuya Yoshizawa [a], Kazuya Yamagata [a, *]

[a] Department of Medical Biochemistry, Faculty of Life Sciences, Kumamoto University, Kumamoto, Japan
[b] Yamamura Project Laboratory, Center for Animal Resources and Development, Institute of Resource Development and Analysis, Kumamoto University, Kumamoto, Japan

ARTICLE INFO

Article history:
Received 9 March 2015
Available online 24 March 2015

Keywords:
Glucokinase
Knockout mouse
Glycogen
Brown adipose tissue
Insulin secretion

ABSTRACT

Glucokinase is expressed principally in pancreatic β-cells and hepatocytes, and catalyzes the phosphorylation of glucose to glucose-6-phosphate, a rate-limiting step of glycolysis. To better understand the roles of hepatic glucokinase, we generated *Gck* knockout mice by ablating liver-specific exon 1b. The knockout mice exhibited impaired glucose tolerance, decreased hepatic glycogen content, and reduced *Pklr* and *Fas* gene expression in the liver, indicating that hepatic glucokinase plays important roles in glucose metabolism. It has also been reported that hepatic glucokinase regulates the expression of thermogenesis-related genes in brown adipose tissue (BAT) and insulin secretion in response to glucose. However, the liver-specific *Gck* knockout mice displayed neither altered expression of thermogenesis-related genes in BAT nor impaired insulin secretion by β-cells under a normal chow diet. These results suggest that chronic suppression of hepatic glucokinase has a small influence on intertissue (liver-to-BAT as well as liver-to-β-cell) metabolic communication.

1. Introduction

Glucokinase (GCK, hexokinase type IV) catalyzes the phosphorylation of glucose to glucose-6-phosphate (G6P), which is a rate-limiting step in glycolysis [1,2]. Glucokinase is characterized by a high K_m for glucose and a lack of allosteric inhibition by G6P compared to hexokinases I–III. Thus, the rate of glucose phosphorylation is directly proportional to blood glucose levels. Glucokinase is expressed principally in pancreatic β-cells and hepatocytes, but is also present in certain hypothalamic neurons and enteroendocrine cells [2]. The *GCK* gene consists of exons 1a, 1b, and 2–10, and two alternate promoters regulate the tissue-specific expression of exons 1a and 1b [3,4]. Exon 1a is expressed in β-cells, enteroendocrine cells, and neuronal cells, whereas exon 1b is expressed in hepatocytes only. In β-cells, glucokinase serves as a glucose sensor and plays a crucial role in the regulation of insulin secretion [5]. Heterozygous inactivating mutations in the *GCK* gene cause a type of maturity-onset diabetes of the young (MODY2), which is characterized by abnormalities in insulin secretion [4,6]. Homozygous inactivating mutations in the *GCK* gene result in a more severe phenotype presenting at birth as permanent neonatal diabetes [7]. In contrast, activating mutations in the *GCK* gene cause hyperinsulinemic hypoglycemia [8].

Liver glucokinase also plays an essential role in controlling blood glucose levels and maintaining cellular metabolic functions [2]. After glucose is taken up by the liver, it is converted to G6P by glucokinase and stored as glycogen. MODY2 patients reportedly have impaired glucose uptake by liver and decreased accumulation of hepatic glycogen [9,10]. Hepatic glucokinase is also required for the proper activation of glycolytic and lipogenic gene expression in the liver [11]. In addition to these hepatic roles of glucokinase, previous studies have shown that this enzyme is involved in metabolic communication between the liver and different tissues. Adenovirus-mediated overexpression of glucokinase in the liver decreased adaptive thermogenesis by downregulating the expression of thermogenesis-related genes in brown adipose tissue (BAT) [12]. In addition, liver-specific glucokinase knockout mice generated by the Cre/loxP system exhibited impaired insulin secretion in

* Corresponding author. Department of Medical Biochemistry, Faculty of Life Sciences, Kumamoto University, 1-1-1 Honjo, Kumamoto, Kumamoto 860-8556, Japan. Fax: +81 96 364 6940.
E-mail address: k-yamaga@kumamoto-u.ac.jp (K. Yamagata).
[1] These authors contributed equally to this work.

http://dx.doi.org/10.1016/j.bbrc.2015.03.097
0006-291X/

response to glucose [13]. These results suggest the presence of intertissue (liver-to-BAT as well as liver-to-β-cell) metabolic pathways.

To understand better the roles of hepatic glucokinase *in vivo*, we generated a new line of *Gck* knockout mice by ablating liver-specific exon 1b. The *Gck* (−/−) mice characterized in the present study exhibited hyperglycemia after glucose load, a defect in hepatic glycogen accumulation, and reduced glycolytic and lipogenic gene expression in the liver. However, these mice displayed neither an insulin secretion defect nor altered expression of thermogenesis-related genes (*Ucp1*, *Pgc1a*, and *Dio2*) in BAT when fed a normal chow diet, suggesting that intertissue regulation by glucokinase is not functional under these conditions. Further studies are necessary to clarify the roles of hepatic glucokinase in intertissue metabolic communication.

2. Materials and methods

2.1. Animals

Construction of the targeting vector and isolation of targeted embryonic stem (ES) cells were carried out using a method described previously [14], except for the use of a 3.86-kb 5′ homologous region upstream and 5.49-kb 3′ homologous region downstream of the ATG codon of exon 1b (Fig. 1A). Chimeric mice were produced by aggregation of ES cells with 8-cell embryos from ICR mice according to a method described previously [14]. Genotyping PCR was performed using a TaKaRa LA PCR Kit with GC buffer (TaKaRa Bio, Inc., Shiga, Japan) according to the manufacturer's instructions. The primer sequences were as follows: forward primer (GTP-F1) and reverse primer (GTP-R1) were 5′-AGGAACATCTCTACTTCCCCAACG-3′ and 5′-TGAGCACACTCTGATTGCCCACC-3′ respectively. The PCR product sizes for the wild-type (WT) and knockout mice were 670 bp and 2597 bp, respectively. All mice were kept under specific-pathogen free conditions in a 12-h light/12-h dark cycle with free access to water and normal chow diet (CE-2; CLEA, Tokyo, Japan) in a temperature-controlled room (22 ± 1–2 °C). All experiments were approved by the Kumamoto University Ethics Committee for Animal Experiments.

2.2. Quantitative RT-PCR

Total RNA was extracted from the liver and BAT using Sepasol-RNAI reagent (Nacalai Tesque, Kyoto, Japan). Quantitative RT-PCR was performed using SYBR Premix Ex Taq II (RR820A; TaKaRa) in an ABI 7300 thermal cycler (Applied Biosystems, Foster City, CA) as described previously [15]. The relative mRNA level of each gene was normalized to that of 18S rRNA. The specific primers used in this study were as follows. *Gck*: forward 5′-ACAAGGAGGGGAGCCCAGTC-3′, reverse 5′-CCCCCACTTTCACCAGCATC-3′; *Pklr*: forward 5′-GGGGTGACCTTGGCATTGAG-3′, reverse 5′-TTACAGCCTCCACGGGGAAA-3′; *Fas*: forward 5′-TCTGGGCCAACCTCATTGGT-3′, reverse 5′-GAAGCTGGGGGTCCATTGTG-3′; *Hk1*: forward 5′-TGCCTCTGGGCTTCACCTTC-3′, reverse 5′-CCACACAGTCGGTGGCTTTG-3′; *Ucp1*: forward 5′-GGCAACAAGACTGACAGTAAAT-3′, reverse 5′-GGCCCTTGTAAACAAAAAATAC-3′; *Pgc1a*: forward 5′-GGCAACAAGAGCTGAA-3′, reverse 5′-GAATAGGGCTGCGTGCATC-3′; *Dio2*: forward 5′-AGTCAAGAAGGTGGCATTCG-3′, reverse 5′-ACAGCTTCCTCCTAGATGCCT-3′; and *18s rRNA*, forward 5′-GGAGAACTCACTGAGCATGA-3′, reverse 5′-CCAGTGGTCTTGGTGTGCTG-3′.

2.3. Immunoblotting

Tissues were lysed in RIPA buffer (50 mM Tris–HCl [pH 8.0], 150 mM NaCl, 0.1% SDS, 1% Nonidet P-40, 5 mM EDTA, 0.5% sodium deoxycholate, 20 mg/mL Na_3VO_4, 10 mM NaF, 1 mM PMSF, 2 mM DTT, and protease inhibitor cocktail [1/100]) using an ultrasonic homogenizer (BRANSON SONIFIER 250; Branson Ultrasonic Corp, Danbury, CT, USA). Pancreatic islets were isolated by the collagenase digestion method [16]. Hypothalami were collected as described previously [17]. Proteins (liver: 20 μg; pancreatic islets: 15 μg; hypothalamus: 100 μg; small intestine: 100 μg) were separated on a 10% polyacrylamide gel using SDS-PAGE and transferred to a PVDF membrane, which was probed with the primary antibodies. After incubation with the secondary antibodies, proteins were visualized using the Chemi-Lumi One Super Reagent (Nacalai Chemical, Kyoto, Japan) and images were captured using an LAS-1000 analyzer (Fujifilm, Tokyo, Japan). Anti-GCK (H-88; Santa Cruz Biotechnology, Santa Cruz, CA, USA) and anti-β-actin (AC-15; Sigma-Aldrich, St. Louis, MO, USA) were used as primary antibodies.

2.4. Metabolic studies

For the measurement of G6P, mice were sacrificed at 3 h after feeding following a 24-h fast. Liver tissue (40 mg) was homogenized in perchloric acid by using a Bioruptor (Diagenode, Denville, NJ, USA) and neutralized with 2 M KOH/0.6 M 2-(N-morpholino) ethanesulfonic acid. After centrifugation at 20,000 × *g* at 4 °C for 10 min, the supernatant was subject to a Glucose-6-Phosphate Colorimetric Assay Kit (Biovision Research Products, Mountain View, CA). Hepatic glycogen content was measured as described [18]. Male mice (9–12-week-old) were fasted for 14 h, and glucose (2 g/kg body weight) was injected intraperitoneally. Glucose levels were measured with a glucose sensor (Glutest Neo Super; Sanwa Kagaku, Nagoya, Japan). Serum insulin levels were measured using a mouse insulin ELISA kit (type S) (Shibayagi Co., Gunma, Japan). For the insulin tolerance test (ITT), fourteen-week-old male mice were injected with regular human insulin after a 4-h fast. Total pancreatic insulin content was measured after extraction by the acid-ethanol method [19]. Rectal temperature was monitored using an electronic thermistor (Model BAT-12; Physitemp, Clifton, NJ, USA) equipped with a rectal probe (RET-3; Physitemp, Clifton, NJ, USA) [20].

2.5. Histological analysis

Pancreas was fixed with buffered 10% formalin at room temperature for 3 days. Hematoxylin/eosin (HE) staining was performed using tissue sections (10 μm thick) of paraffin-embedded blocks. To analyze islet mass, sections of paraffin-embedded pancreatic tissues were cut at 100-μm intervals [21]. HE-stained islet images were captured by an all-in-one fluorescent microscope (BZ-9000; KEYENCE, Tokyo, Japan) and the islet areas (μm^2) were measured using ImageJ software.

2.6. Statistical analysis

Data are shown as means ± standard error. The significance of differences was assessed using the unpaired t-test, and $p < 0.05$ was considered to indicate statistical significance.

3. Results

3.1. Generation of novel liver-specific Gck-deficient mice

After electroporation with the targeting vectors, 176 neo-resistant clones were screened for targeted recombination by Southern blot analysis. Using a neo probe, 9 clones gave 9.4- or 11.0-kb bands when digested with *Kpn*I or *Bgl*II, respectively (Fig. 1A). Of

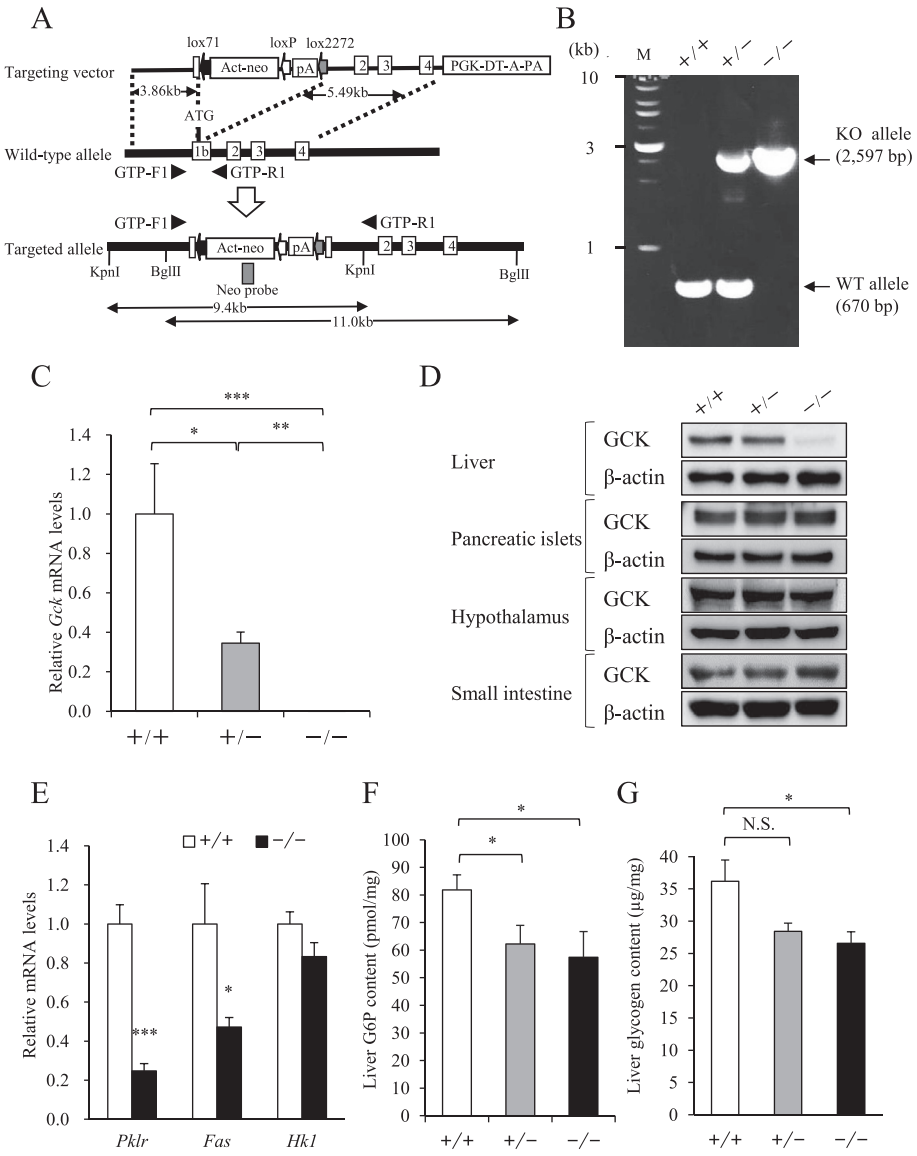

Fig. 1. Generation of liver-specific *Gck* knockout mice. (A) Targeting vector construction. (B) PCR was performed for genotyping. The PCR product for the wild-type (WT) allele was 670 bp, while the knockout (KO) allele generated a 2597 bp PCR product. (C) Expression levels of *Gck* exon 1b transcript in the liver of male *Gck* (+/+), *Gck* (+/−), or *Gck* (−/−) mice (n = 4–6, 16 weeks old) were evaluated by quantitative RT-PCR. The value of each gene was normalized to that of 18S rRNA. Data are the means ± standard error (SE). *p < 0.05; **p < 0.01; ***p < 0.001. (D) Glucokinase protein expression in the liver and other tissues. β-Actin was used as a loading control. (E) Expression of hepatic genes in male *Gck* (+/+) and *Gck* (−/−) mice (n = 6 each). Mice were refed for 18 h after 24-h fasting. (F, G) G6P (F) and glycogen (G) content in the liver of male *Gck* (+/+) (blank bars), *Gck* (+/−) (gray bars), or *Gck* (−/−) (filled bars) mice (n = 4–7). Mice were refed for 3 h after 24-h fasting. The value of each gene was normalized to that of 18S rRNA. Data are shown as the means ± SE. *p < 0.05; **p < 0.01; ***p < 0.001; N.S., not significant.

the 9 ES-targeted clones, 1 showed germline transmission. F1 mice were bred with C57BL/6 mice. Genotypes of the mice were assessed by PCR (Fig. 1B). Three alleles were inherited in a Mendelian fashion and were phenotypically indistinguishable (data not shown). We next examined the transcription of exon 1b by quantitative RT-PCR. As shown in Fig. 1C, *Gck* mRNA expression was significantly decreased in the liver of *Gck* (+/−) mice compared with control mice and was nearly absent in the liver of *Gck* (−/−) mice. In spite of the almost complete lack of exon 1b transcription, western blot analysis revealed that Gck protein was still detectable at low levels (about 10% of control) in the liver of *Gck* (−/−) mice (Fig. 1D). Compensatory expression of β-cell-specific exon 1a transcription was not observed in the liver of *Gck* (−/−) mice (data not shown). The human *GCK* gene has an additional liver-specific exon 1c, and a minor transcript encoded by exons 1c and 2–10 has been detected in the liver [4]. Although exon 1c has not been identified in the mouse *Gck* gene [22], the residual signal obtained in the liver of *Gck* (−/−) mice may due to glucokinase protein encoded by exons 1c–10. In addition, the possible expression of the recently identified ADP-dependent glucokinase [23] cannot be ruled out. Expression of Gck protein in pancreatic islets, hypothalamus, and small intestine was unchanged in the *Gck* (−/−) mice (Fig. 1D).

3.2. Glucokinase regulates gene expression and glycogen synthesis in the liver

Hepatic glucokinase is required for the normal expression of *Pklr* and *Fas* mRNA after refeeding [11]. As reported previously, the expression of both genes was significantly decreased in the liver of *Gck* (−/−) mice (Fig. 1E). Hepatic glycogen is synthesized by a direct

pathway (glucose→G6P→glycogen) and an indirect (gluconeogenic) (3-carbon units→G6P→glycogen) pathway [9]. Impaired glycogen synthesis after meals has been reported in patients with MODY2 [9]. Consistently, both G6P and glycogen levels were decreased in the livers of 3-h refed *Gck* (+/−) and *Gck* (−/−) mice compared with control mice (Fig. 1F and G), indicating that normal glycogen levels cannot be maintained by hexokinase (Fig. 1E) or the indirect pathway in the absence of glucokinase.

3.3. Impact of hepatic glucokinase on gene expression in BAT and adiposity

A recent study revealed that hepatic glucokinase overexpression in the liver of chow-fed C57BL/6 mice suppresses sympathetic nerve activity to BAT, thereby downregulating the expression of the thermogenesis-related *Ucp1*, *Pgc1a*, and *Dio2* genes and modulating predisposition to obesity [12]. Conversely, hepatic glucokinase knockdown in high-fat diet (HFD)-fed C57BL/6 mice attenuated weight gain with increased expression of *Ucp1*, *Pgc1a*, and *Dio2* in BAT [12]. Thus, we investigated the expression of these genes in BAT of *Gck* (−/−) mice. However, there was no significant difference in the expression levels of *Ucp1*, *Pgc1a*, and *Dio2* in BAT among the 3 groups (Fig. 2A) and the body temperature was also similar (Fig. 2B). In addition, there was no change in body weight or adipose tissue (white adipose tissue [WAT] and BAT) weight (Fig. 2C and D). Therefore, the impact of the chronic suppression of hepatic glucokinase on BAT thermogenesis and adiposity is small, if any, in mice fed normal chow.

3.4. Impact of hepatic glucokinase on glucose tolerance and insulin secretion

Postic et al. generated liver-specific glucokinase knockout mice by breeding mice carrying the albumin (Alb)-Cre transgene with $gk^{lox/lox}$ mice containing 2 loxP sites flanking exons 9 and 10 [13]. The resultant liver-specific glucokinase knockout mice displayed increased glucose concentrations under both fasted and fed conditions. In addition, these mice exhibited a profound defect of glucose-stimulated insulin secretion during hyperglycemia [13].

Thus, we investigated glucose tolerance and insulin secretion ability in our *Gck* knockout mice. As shown in Fig. 3A, non-fasting glucose concentrations did not differ among the 3 alleles. However, an intraperitoneal glucose tolerance test revealed that *Gck* (+/−) animals showed a significant increase in blood glucose concentrations when compared to WT mice at 30 min and 60 min after glucose load (Fig. 3B). *Gck* (−/−) mice exhibited further increased glucose concentrations when compared to *Gck* (+/+) and *Gck* (+/−) animals (Fig. 3B), indicating that *Gck* (−/−) and *Gck* (+/−) mice were glucose intolerant. Previous studies suggested that hepatic glucokinase deficiency leads to insulin resistance [2,13]; however, non-fasting insulin levels were similar between our *Gck* (−/−) and control mice (data not shown). An ITT did not reveal any significant difference between *Gck* (−/−) and *Gck* (+/+) mice, suggesting the peripheral insulin sensitivity of our mutant mice was normal (Fig. 3C). Fasting insulin levels were also similar among the groups (Fig. 3D). In contrast to the previous study, the acute phase of insulin secretion (15 min and 30 min after glucose load) was similar

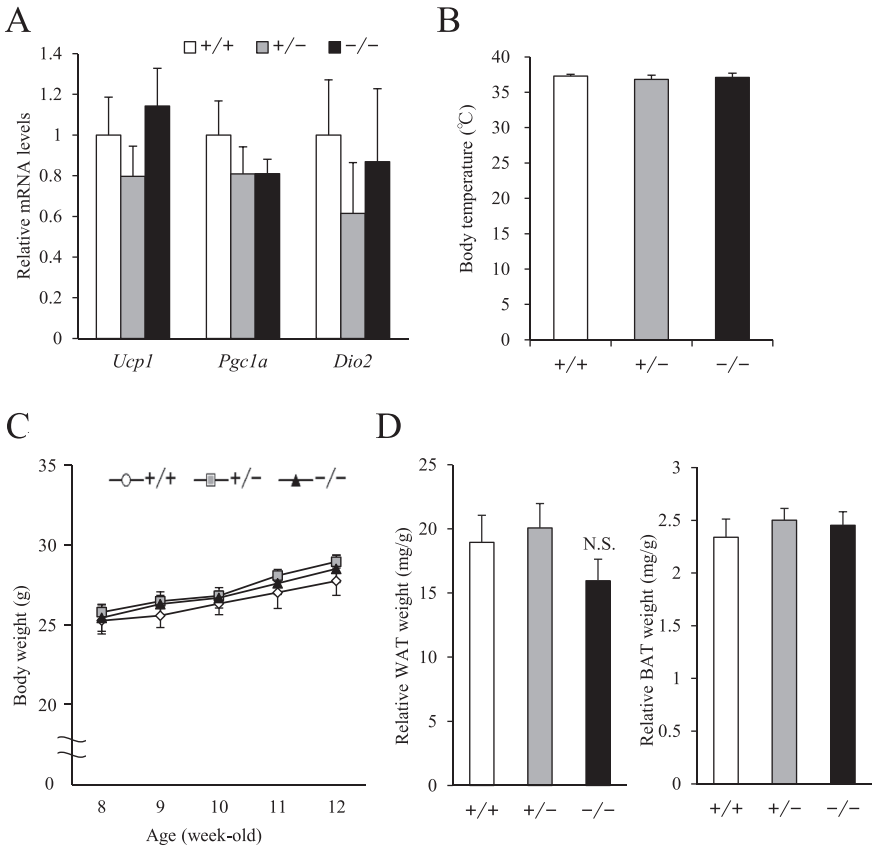

Fig. 2. Effect of hepatic glucokinase on gene expression in BAT and adiposity. (A) Expression of *Ucp1*, *Pgc1a*, and *Dio2* mRNA in BAT of male *Gck* (+/+, blank bars), *Gck* (+/−, gray bars), or *Gck* (−/−, filled bars) mice (n = 5). (B) Body temperature of the mice (n = 3) was measured during the *ad libitum*-fed condition. (C) Body weight of male *Gck* (+/+, circles), *Gck* (+/−, squares), or *Gck* (−/−, triangles) mice (n = 6–9). (D) Relative weight of white adipose tissue (WAT, left) and brown adipose tissue (BAT, right) of male *Gck* (+/+, +/−, and −/−) mice (n = 15–19). Data are shown as the means ± SE. N.S., not significant.

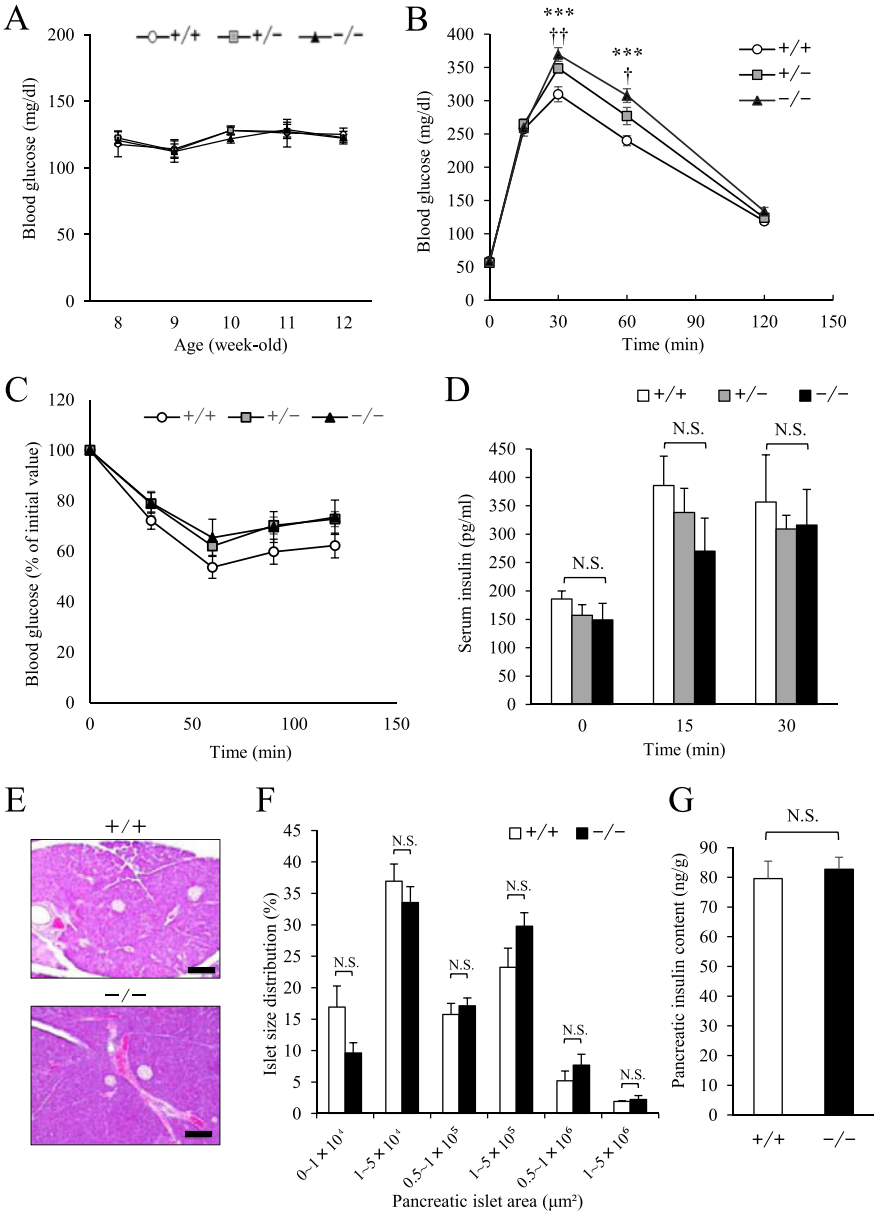

Fig. 3. Role of hepatic glucokinase in glucose metabolism and insulin secretion. (A) Blood glucose levels of *ad libitum*-fed male *Gck* (+/+, circles), *Gck* (+/−, squares), or *Gck* (−/−, triangles) mice (n = 6–9). (B) Intraperitoneal glucose tolerance test in male *Gck* (+/+, +/−, and −/−) mice (n = 10–13). ***p < 0.001 for *Gck* (+/+) versus *Gck* (−/−) mice; †p < 0.05 and ††p < 0.01 for *Gck* (+/+) versus *Gck* (+/−) mice. (C) Insulin tolerance test in male *Gck* (+/+, +/−, and −/−) mice (n = 8–9). Values are expressed as a percentage of the initial value. (D) Plasma insulin levels before and after glucose injection (n = 4–5). (E) Hematoxylin/eosin staining of the pancreas in male *Gck* (+/+, upper; and −/−, lower) mice. Scale bar, 100 μm. (F) Distribution of pancreatic islet areas in *Gck* (+/+, blank bars; and −/−, filled bars) mice. In *Gck* (+/+ and −/−) mice, 730 and 815 islets were measured, respectively. (G) Insulin content of the whole pancreas in *Gck* (+/+ and −/−) mice (n = 6–7). Data are shown as the means ± SE. *p < 0.05; **p < 0.01; ***p < 0.001; N.S., not significant.

among the 3 groups (Fig. 3D). Histological analysis revealed normal islet architecture in *Gck* (−/−) knockout mice (Fig. 3E). Quantitative analysis revealed no significant difference in islet size between *Gck* (−/−) and WT mice (Fig. 3F). Furthermore, the pancreatic insulin content of *Gck* (−/−) mice was similar to that of control mice (Fig. 3G). These results indicate that neither insulin secretion, insulin content, nor islet architecture was affected by hepatic glucokinase deficiency.

4. Discussion

Our liver-specific *Gck* (−/−) mice and another line of liver-specific mice [13] exhibited impaired glucose tolerance. Furthermore, both knockout mice showed decreased hepatic glycogen content and reduced *Pklr* and *Fas* gene expression in the liver [11]. However, there were several differences between our mutant mice and theirs. First, their mice showed a significant increase of blood glucose levels in both the fed and fasting states. In contrast, there were no significant difference in blood glucose levels between our *Gck* (−/−) and *Gck* (+/+) mice. Second, they reported the presence of hyperinsulinemia (indicative of insulin resistance) in their knockout mice. The insulin levels and insulin tolerance in our *Gck* (−/−) knockout mice were indistinguishable from those of control mice. Third, glucose-induced insulin secretion in their liver-specific knockout mice during hyperglycemic clamp experiments was markedly decreased; however, insulin secretion was normal after intraperitoneal injection of glucose in our *Gck* (−/−) mice. Postic et al. used $gk^{lox/lox}$ mice as a control of glucokinase knockout mice

($gk^{lox/lox}$ + Alb-Cre), but $gk^{lox/lox}$ mice themselves exhibited significantly increased blood glucose concentrations when compared to WT mice due to the insertion of the loxP sequences. Although we have no adequate explanation for these differences, the chronic hyperglycemia of $gk^{lox/lox}$ mice may have contributed to the different findings of the two studies.

A recent study revealed that hepatic glucokinase regulates thermogenesis-related gene expression in BAT [12]. In addition, hepatic glucokinase knockdown in HFD-fed C57BL/6 mice attenuated weight gain with increased expression of *Ucp1*, *Pgc1a*, and *Dio2* in BAT. However, gene expression was unaffected and body weight was also unchanged in our *Gck* (−/−) mice. Different experimental conditions (chronic suppression versus acute suppression) or different dietary conditions (normal chow versus HFD) may have contributed to these different findings.

In the present study, we generated novel liver-specific glucokinase knockout mice and demonstrated the determinant roles of glucokinase in hepatic glycogen synthesis and glycolysis and lipid synthesis-related gene expression. It has been also reported that hepatic glycogen content regulates nerve-mediated lipolysis in WAT [24]. Further studies of these liver-specific glucokinase knockout mice could be useful to clarify intertissue metabolic communication via glucokinase.

Conflict of interest

The authors declare that there are no conflicts of interest.

Acknowledgments

We thank Professor T. Fukuda (Kumamoto University) for technical assistance with preparing hypothalamus. This work was supported by a Grant-in-Aid for Scientific Research (B) (25293212), a grant from the Novo Nordisk Insulin Research Foundation to Kazuya Yamagata, and a Grant-in-Aid for Scientific Research (S) (21220010) to Ken-ichi Yamamura.

Transparency document

Transparency document related to this article can be found online at http://dx.doi.org/10.1016/j.bbrc.2015.03.097.

References

[1] F.M. Matschinsky, Assessing the potential of glucokinase activators in diabetes therapy, Nat. Rev. Drug Discov. 8 (2009) 399–416.
[2] P.B. Iynedjian, Molecular physiology of mammalian glucokinase, Cell. Mol. Life Sci. 66 (2009) 27–42.
[3] P.B. Iynedjian, Mammalian glucokinase and its gene, Biochem. J. 293 (1993) 1–13.
[4] K.K. Osbak, K. Colclough, C. Saint-Martin, N.L. Beer, C. Bellanné-Chantelot, S. Ellard, A.L. Gloyn, Update on mutations in glucokinase (GCK), which cause maturity-onset diabetes of the young, permanent neonatal diabetes, and hyperinsulinemic hypoglycemia, Hum. Mutat. 30 (2009) 1512–1526.
[5] F.M. Matschinsky, Regulation of pancreatic beta-cell glucokinase: from basics to therapeutics, Diabetes 51 (2002) S394–S404.
[6] M.M. Byrne, J. Sturis, K. Clément, N. Vionnet, M.E. Pueyo, M. Stoffel, J. Takeda, P. Passa, D. Cohen, G.I. Bell, et al., Insulin secretory abnormalities in subjects with hyperglycemia due to glucokinase mutations, J. Clin. Invest 93 (1994) 1120–1130.
[7] P.R. Njølstad, O. Søvik, A. Cuesta-Muñoz, L. Bjørkhaug, O. Massa, F. Barbetti, D.E. Undlien, C. Shiota, M.A. Magnuson, A. Molven, F.M. Matschinsky, G.I. Bell, Neonatal diabetes mellitus due to complete glucokinase deficiency, N. Engl. J. Med. 344 (2001) 1588–1592.
[8] B. Glaser, P. Kesavan, M. Heyman, E. Davis, A. Cuesta, A. Buchs, C.A. Stanley, P.S. Thornton, M.A. Permutt, F.M. Matschinsky, K.C. Herold, Familial hyperinsulinism caused by an activating glucokinase mutation, N. Engl. J. Med. 338 (1998) 226–230.
[9] G. Velho, K.F. Petersen, G. Perseghin, J.H. Hwang, D.L. Rothman, M.E. Pueyo, G.W. Cline, P. Froguel, G.I. Shulman, Impaired hepatic glycogen synthesis in glucokinase-deficient (MODY-2) subjects, J. Clin. Invest 98 (1996) 1755–1761.
[10] H. Sakura, R. Kawamori, M. Kubota, T. Morishima, T. Kamada, Y. Akanuma, Y. Yazaki, T. Kadowaki, Glucokinase gene mutation and impaired glucose uptake by liver, Lancet 341 (1993) 1532–1533.
[11] R. Dentin, J.P. Pégorier, F. Benhamed, F. Foufelle, P. Ferré, V. Fauveau, M.A. Magnuson, J. Girard, C. Postic, Hepatic glucokinase is required for the synergistic action of ChREBP and SREBP-1c on glycolytic and lipogenic gene expression, J. Biol. Chem. 279 (2004) 20314–20326.
[12] S. Tsukita, T. Yamada, K. Uno, K. Takahashi, K. Kaneko, Y. Ishigaki, J. Imai, Y. Hasegawa, S. Sawada, H. Ishihara, Y. Oka, H. Katagiri, Hepatic glucokinase modulates obesity predisposition by regulating BAT thermogenesis via neural signals, Cell. Metab. 16 (2012) 825–832.
[13] C. Postic, M. Shiota, K.D. Niswender, T.L. Jetton, Y. Chen, J.M. Moates, K.D. Shelton, J. Lindner, A.D. Cherrington, M.A. Magnuson, Dual roles for glucokinase in glucose homeostasis as determined by liver and pancreatic beta cell-specific gene knock-outs using Cre recombinase, J. Biol. Chem. 274 (1999) 305–315.
[14] G. Zhao, Z. Li, K. Araki, K. Haruna, K. Yamaguchi, M. Araki, M. Takeya, Y. Ando, K. Yamamura, Inconsistency between hepatic expression and serum concentration of transthyretin in mice humanized at the transthyretin locus, Genes. Cells 13 (2008) 1257–1268.
[15] K. Fukui, Q. Yang, Y. Cao, N. Takahashi, H. Hatakeyama, H. Wang, J. Wada, Y. Zhang, L. Marselli, T. Nammo, K. Yoneda, M. Onishi, S. Higashiyama, Y. Matsuzawa, F.J. Gonzalez, G.C. Weir, H. Kasai, I. Shimomura, J. Miyagawa, C.B. Wollheim, K. Yamagata, The HNF-1 target collectrin controls insulin exocytosis by SNARE complex formation, Cell. Metab. 2 (2005) 373–384.
[16] Y. Sato, M. Hatta, M.F. Karim, T. Sawa, F.Y. Wei, S. Sato, M.A. Magnuson, F.J. Gonzalez, K. Tomizawa, T. Akaike, T. Yoshizawa, K. Yamagata, Anks4b, a novel target of HNF4α protein interacts with GRP78 protein and regulates endoplasmic reticulum stress-induced apoptosis in pancreatic β-cells, J. Biol. Chem. 287 (2012) 23236–23245.
[17] X. Zhang, G. Zhang, H. Zhang, M. Karin, H. Bai, D. Cai, Hypothalamic IKKbeta/NF-kappaB and ER stress link overnutrition to energy imbalance and obesity, Cell 135 (2008) 61–73.
[18] J.V. Passonneau, V.R. Lauderdale, A comparison of three methods of glycogen measurement in tissues, Anal. Biochem. 60 (1974) 405–412.
[19] K. Yamagata, T. Nammo, M. Moriwaki, A. Ihara, K. Iizuka, Q. Yang, T. Satoh, M. Li, R. Uenaka, K. Okita, H. Iwahashi, Q. Zhu, Y. Cao, A. Imagawa, Y. Tochino, T. Hanafusa, J. Miyagawa, Y. Matsuzawa, Mutant hepatocyte nuclear factor-1α in pancreatic β-cells causes abnormal islet architecture with decreased expression of E-cadherin, reduced β-cell proliferation, and diabetes, Diabetes 51 (2002) 114–123.
[20] T. Yoshizawa, M.F. Karim, Y. Sato, T. Senokuchi, K. Miyata, T. Fukuda, C. Go, M. Tasaki, K. Uchimura, T. Kadomatsu, Z. Tian, C. Smolka, T. Sawa, M. Takeya, K. Tomizawa, Y. Ando, E. Araki, T. Akaike, T. Braun, Y. Oike, E. Bober, K. Yamagata, SIRT7 controls hepatic lipid metabolism by regulating the ubiquitin-proteasome pathway, Cell. Metab. 19 (2014) 712–721.
[21] A. Miura, K. Yamagata, M. Kakei, H. Hatakeyama, N. Takahashi, K. Fukui, T. Nammo, K. Yoneda, Y. Inoue, F.M. Sladek, M.A. Magnuson, H. Kasai, J. Miyagawa, F.J. Gonzalez, I. Shimomura, Hepatocyte nuclear factor-4alpha is essential for glucose-stimulated insulin secretion by pancreatic beta-cells, J. Biol. Chem. 281 (2006) 5246–5257.
[22] K. Ishimura-Oka, M. Nakamuta, M.J. Chu, M. Sullivan, L. Chan, K. Oka, Partial structure of the mouse glucokinase gene, Genomics 29 (1995) 751–754.
[23] R.S. Ronimus, H.W. Morgan, Cloning and biochemical characterization of a novel mouse ADP-dependent glucokinase, Biochem. Biophys. Res. Commun. 315 (2004) 652–658.
[24] Y. Izumida, N. Yahagi, Y. Takeuchi, M. Nishi, A. Shikama, A. Takarada, Y. Masuda, M. Kubota, T. Matsuzaka, Y. Nakagawa, Y. Iizuka, K. Itaka, K. Kataoka, S. Shioda, A. Niijima, T. Yamada, H. Katagiri, R. Nagai, N. Yamada, T. Kadowaki, H. Shimano, Glycogen shortage during fasting triggers liver-brain-adipose neurocircuitry to facilitate fat utilization, Nat. Commun. 4 (2013) 2316.